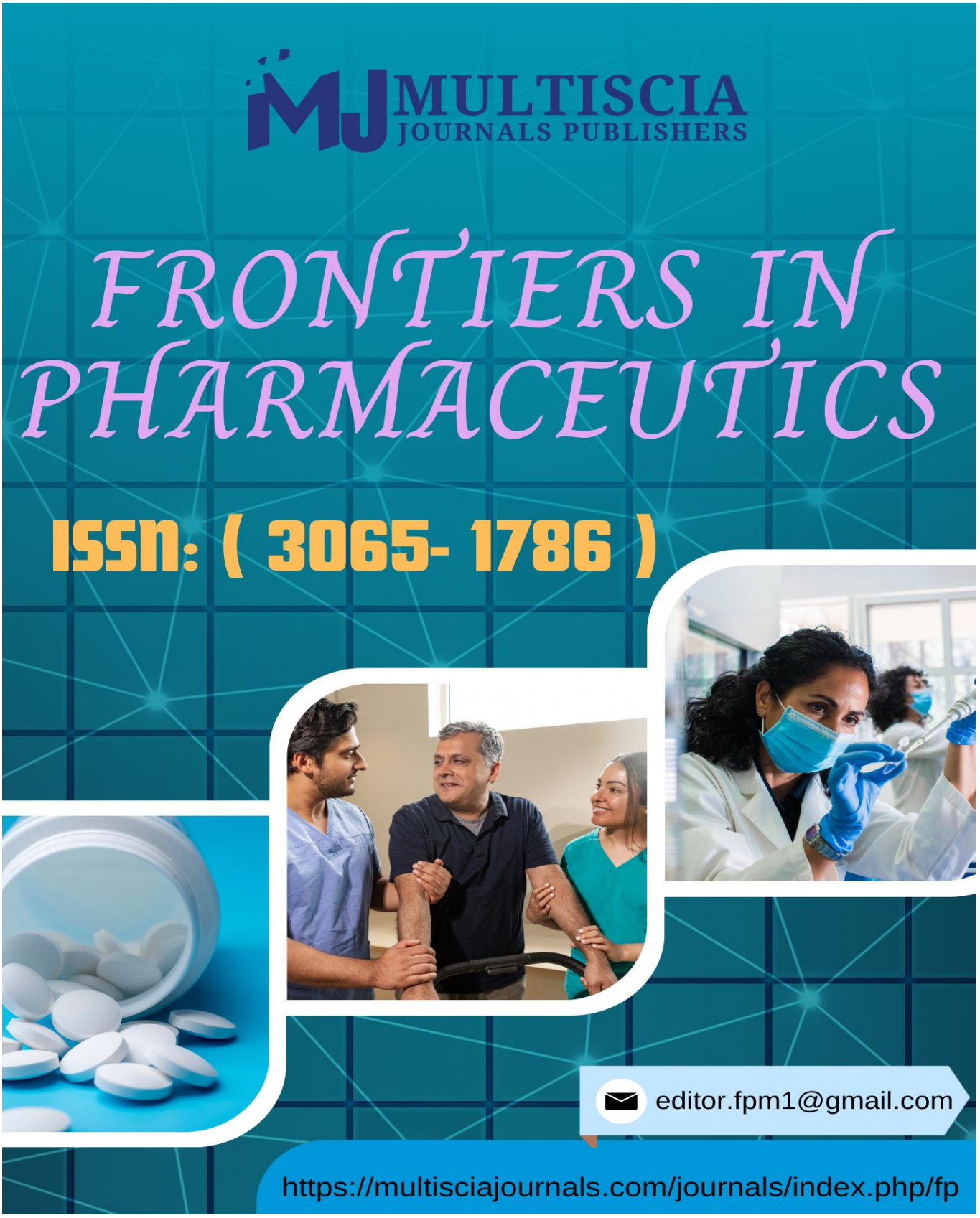
MULTISCIA
JOURNALS PUBLISHERS
FRONTIERS IN PHARMACEUTICS
ISSN: ( 3065- 1786 )
editor.fpm1@gmail.com
https://multisciajournals.com/journals/index.php/fp

**Frontiers in Pharmaceutics**
**Volume 1 Issue 2 2025**

# Characterization of the Freeze-Dried $\alpha$-Glucosidase Inhibitor/Cyclodextrin Complex

D Vishnyakova, R Rodriguez
Department of **Pharmaceutics**

**Article Info**

**Received: 24-02-2025 Revised:22-03-2025 Accepted:09-04-2025 Published:21-04-2025**

## 1. Introduction

In developed nations, the prevalence of diabetes has risen recently. Smoking, poor nutrition, and inactivity have all been linked to this, and diabetes has emerged as a significant contributor to the rising death rate [1]. The International Diabetes Federation research states that 415 million people worldwide have diabetes in 2015 and that the number of people with the disease is still rising. Because of this, there has been an increase in interest in treating prediabetes by keeping blood glucose levels below those necessary for a diabetes diagnosis in order to stop the onset of full-blown diabetes.
Currently utilized as food additives, cyclodextrins (CDs) are cyclic dextrins. It has recently been reported that $\alpha$CD lowers blood sugar levels. In particular, $\alpha$CD decreased blood sugar rises [3] and pancreatic amylase activity [2]. Additionally, by being a part of a complex, CDs solubilize, stabilize, and conceal medications. For instance, the creation of an inclusion complex consisting of hydroxypropyl-$\beta$CD and the sparingly soluble antifungal drug itraconazole [4] enhanced the solubility of the medication. Furthermore, the drug's stability was enhanced by the creation of an inclusion complex consisting of limaprost, a prostaglandin E1 derivative that is unstable to moisture, and $\alpha$-cyclodextrin [5]. Additionally, cyclodextrin masking reduced the bitterness of a medication [6].
Acarbose (AB), voglibose (VB), and miglitol (MT) are the $\alpha$-glucosidase inhibitors that are currently on the market. For type 2 diabetes, AB, VB, and MT are employed as treatment agents. Among these, AB suppresses the activities of $\alpha$-amylase and $\alpha$-glucosidase. Furthermore, because VB and MT have a greater $\alpha$-glucosidase inhibitory activity than AB, they are frequently employed in therapeutic settings. MT is distinct from the other two medications in that it is rapidly absorbed in the top portion of the small intestine. Beginning thirty minutes after a meal and lasting until two hours after a meal, this trait inhibits the increase in blood glucose levels. MT is especially good in preventing the rise in blood sugar that occurs one hour after eating.
In order to create a formulation that would have an additive synergistic inhibitory impact on blood glucose increase by building a complex with $\alpha$CD, this work concentrated on MT. This report's inclusion

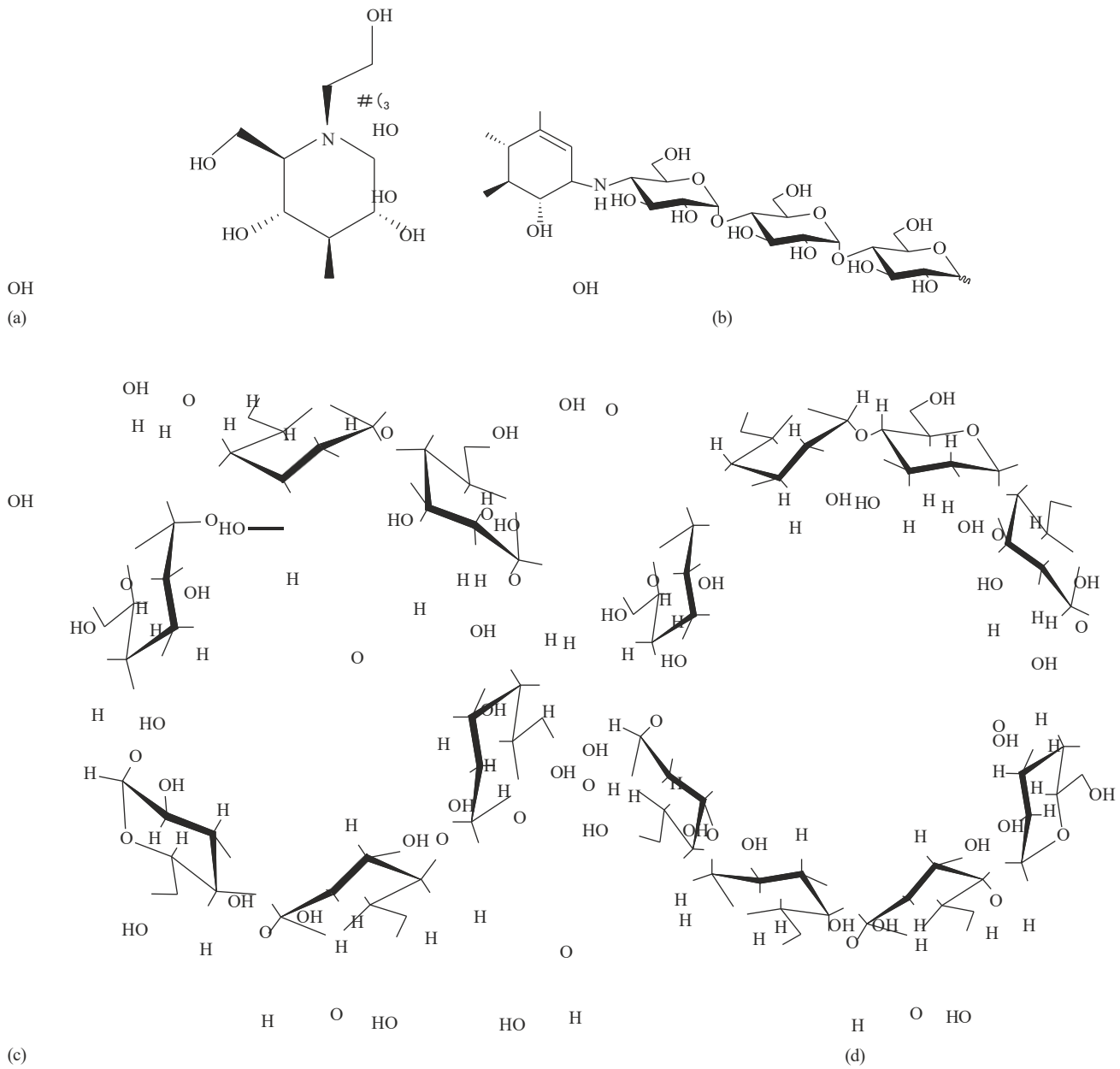


FIGURE 1: Chemical structures of (a) miglitol, (b) acarbose, (c) $\alpha$CD, (d) $\gamma$CD.

complexes with MT were prepared using $\alpha$CD and $\gamma$CD. In addition, the addictive effect of $\alpha$CD and $\gamma$CD with $\alpha$-glucosidase inhibitors was evaluated.

## 2. Materials and Methods

3. Both $\alpha$CD and $\gamma$CD were used to create complexes with MT. Furthermore, the addictive potential of CD and CD combined with glucosidase inhibitors was assessed.

2. Supplies and Procedures
2.1. Supplies. After being donated by Cyclo Chem Co., Ltd. (Tokyo, Japan), $\alpha$CD and $\gamma$CD were kept for seven days before to usage at 40°C and 82% relative humidity. SANWA KAGAKU KENKYUSHO Co., Ltd. contributed MT (Figure 1). Wako Pure Chemical Industries, Ltd. supplied all additional chemicals, which were of analytical quality.

2.2. Techniques
2.2.1. Physical Mixture Preparation. MT/$\alpha$CD and MT/$\gamma$CD were blended for one minute using a vortex mixer to create a physical mixture (PM) of the two compounds at a molar ratio of 1/1.
2.2.2. Freeze-Dried Product Preparation. The process of freeze-drying was used to create complexes. Both MT/$\alpha$CD = 1/1 and MT/$\gamma$CD = 1/1 combinations were dissolved.

Prefrozen at -30°C or lower in 100 milliliters of filtered water. The prefrozen product was then freeze-dried for 24 hours in a vacuum freeze-dryer (ALS Co., Ltd.'s FZ-6 type) to create the freeze-dried product (FD).
2.2.3. PXRD, or powder X-ray diffraction. An X-ray diffractometer (MiniFlex II, Rigaku) with Cu radiation, a scan range of $2\theta$ = 5–40∘, and a scan rate of 4∘/min was used to perform powder X-ray diffraction. A NaI scintillation counter connected to a discriminator was used to measure the diffraction intensities.
2.2.4. Differential Thermal Analyzer/Thermogravimetry. A thermogravimetry/differential thermal analyzer (Thermo plus Evo, Rigaku) was used to examine the samples' thermal behavior at a nitrogen flow rate of 200 mL/min. The samples were heated from 30°C to 350°C at a scanning rate of 5.0°C per minute.
2.2.5. Spectrometry of Near Infrared (NIR) Absorption. A Fourier transform type near infrared spectrometer (Buchi N-500: Nippon Buchi) was used to fill out each sample, with a measurement wavelength of

**4.** 10000–4000 cm−1, an 8 s measurement duration, and a 25∘C measurement temperature with a 1 nm optical path interval.

3.1.1. NMR Spectroscopy of 1H-1H Nuclear Overhauser Effect Spectroscopy (NOESY). Using a cold probe running at 699.6 MHz and a D2O solution, an NMR spectrometer (Varian NMR System 700NB, Agilent) was used to perform two-dimensional (2D) NOESY NMR spectroscopy and selective 1D-NMR spectroscopy. A temperature of 298 K, a pulse width of 90∘, a relaxation delay of 0.267 s, a mixing time of 4.500 s, a fixed delay of 1.500 s, and an acquisition time of 7.0 $\mu$s were the parameters used for the measurement.

3.1.2. Inhibition Test of $\alpha$-glucosidase activity. 600 $\mu$L of 0.1 mol/L maleate buffer (pH 6.0) and 100 microliters of each test solution (MT, $\alpha$CD, $\gamma$CD, PM (MT/$\alpha$CD), PM (MT/$\gamma$CD), FD (MT/$\alpha$CD), and FD (MT/$\gamma$CD)) were added to 100 $\mu$L of a substrate solution (1% maltose). After that, 200 $\mu$L of $\alpha$-glucosidase solution (both active and inactive) was added, and the mixture was incubated for 60 minutes at 37°C to enable a $\alpha$-glucosidase reaction. The solution was heated to 100°C for 15 minutes to halt the process. A 96-well microplate was then filled with 10 $\mu$L of the reaction solution, 200 $\mu$L

of Gluest CII-Test Wako coloring reagent (Wako Pure Chemical Industries, Ltd.), and the mixture was incubated for five minutes at 37∘C. Following incubation, the absorbance was measured at a wavelength of 505 nm using a microplate reader (Spectra Max 190®, Molecular Devices Japan Ltd.). 20 mL of 0.1 mol/L maleic acid buffer solution (pH 6.0) was added to 2.0 g of rat acetone powder (intestinal acetone powder from rats, Sigma-Aldrich), and the mixture was homogenized for one minute. After centrifuging the mixture, the supernatant was utilized as an active solution for $\alpha$-glucosidase. To create an inert liquid, this solution was also heated for 15 minutes at 100°C. The inactive solution served as a negative control, whereas the $\alpha$-glucosidase active solution served as a positive control. Acarbose served as the control agent for the test solution. Acarbose's IC50 value was determined using dose-response curves, which are not included in this study. The findings showed that acarbose's IC50 value was 87 $\mu$g/mL, which was in close agreement with the value that Yang et al. [7] had reported. Therefore, the ratio of 100 mg of one dose of acarbose to 50 mg of one dose of MT was used to determine the MT concentration. To match that of MT alone, the concentrations of PM (MT/$\alpha$CD), PM (MT/$\gamma$CD), FD (MT/$\alpha$CD), and FD (MT/$\gamma$CD) were changed. Additionally, the concentration of FD (MT/CD) and PM (MT/CD) was equal to the concentration of $\alpha$CD, and the concentration of $\gamma$CD was equal to the concentration of PM (MT/CD) and FD (MT/CD). The following formula was used to determine the rate of inhibition of $\alpha$-glucosidase activity: $\alpha$-glucosidase inhibition percentage = $100 - (C - D) \times 100$, (1) where $A$ represents the positive control's glucose concentration, $B$ represents the negative control's glucose concentration, and $C$ is the concentration of glucose that is achieved by mixing the test solution with the positive control, and the concentration of glucose that is obtained by mixing the test solution with the negative control is denoted by $D$.

3.1.3. Inhibition of N►►-Amylase Activity Test. 450 $\mu$L of a substrate solution (0.5% starch aqueous solution) was mixed with 50 microliters of each test solution (MT, $\alpha$CD, $\gamma$CD, PM (MT/$\alpha$CD), PM (MT/$\gamma$CD), FD (MT/$\alpha$CD, and FD (MT/$\gamma$CD)) and 400 $\mu$L of phosphate buffered saline (pH 7.4). To execute a $\alpha$-amylase reaction, 100 $\mu$L of $\alpha$-amylase solution (active solution, inactive solution) was then added, and the combination was incubated for 20 minutes at 37∘C. The reaction was then stopped by adding 500 $\mu$L of DSN reagent (1% 3,5-dinitrosalicylic acid and 12% potassium sodium tartrate in 0.4 mol/L NaOH) to the incubated solution and heating it to 100∘C for 15 minutes. After that, 200 $\mu$L of the reaction solution was poured into a 96-well microplate, and a microplate reader (Spectra Max 190, Molecular Devices Japan KK) was used to measure the absorbance using ELISA at a wavelength of 540 nm. 100 mL of phosphate buffered saline was added to 16.5 mg of porcine pancreatic-derived $\alpha$-amylase (19.5 units amylase/mg, SIGMA). Following a 10-minute ultrasonic treatment, the mixture was centrifuged, and the supernatant was utilized as an active solution of amylase. To create an inert liquid, this solution was also heated for 15 minutes at 100°C. The inactive solution served as a negative control, whereas the $\alpha$-amylase active solution served as a positive control. Acarbose was employed as a control agent for the test solution. Acarbose's IC50 value was determined using dose-response curves, which are not included in this study. The findings showed that acarbose's IC50 value was 20 $\mu$g/mL, which was in close agreement with the number Wickramaratne et al. [8] had reported. Therefore, the ratio of 100 mg of one dose of acarbose to 50 mg of one dose of MT was used to determine the MT concentration. To match that of MT alone, the concentrations of PM (MT/$\alpha$CD), PM (MT/$\gamma$CD), FD (MT/$\alpha$CD), and FD (MT/$\gamma$CD) were changed. Furthermore, the concentration of FD (MT/$\alpha$CD) and PM (MT/$\alpha$CD) was equal to the concentration of $\alpha$CD, and the concentration of $\gamma$CD was equal to the concentration of PM (MT/$\gamma$CD) and FD (MT/$\gamma$CD). The following formula was used to determine the rate of inhibition of $\alpha$-amylase activity:

$\alpha$-Amylase Inhibition% = 100 − ($C$− $D$) × 100, (2) where $A$ represents the concentration of glucose in the positive control, $B$ represents the concentration of glucose in the negative control, $C$ represents the concentration of glucose obtained by mixing the test solution with the positive control, and $D$ represents the concentration of glucose obtained by mixing the test solution with the negative control.

4. Findings and Conversation

4.1. PXRD Analysis. The crystalline state of MT and CDs in the FD (MT/$\alpha$CD) and FD (MT/$\gamma$CD) preparations was investigated using PXRD (Figure 2). Characteristic diffraction peaks at $2\theta$ = 15.5∘ and 19.2∘ were displayed by intact MT.

*4.1.*

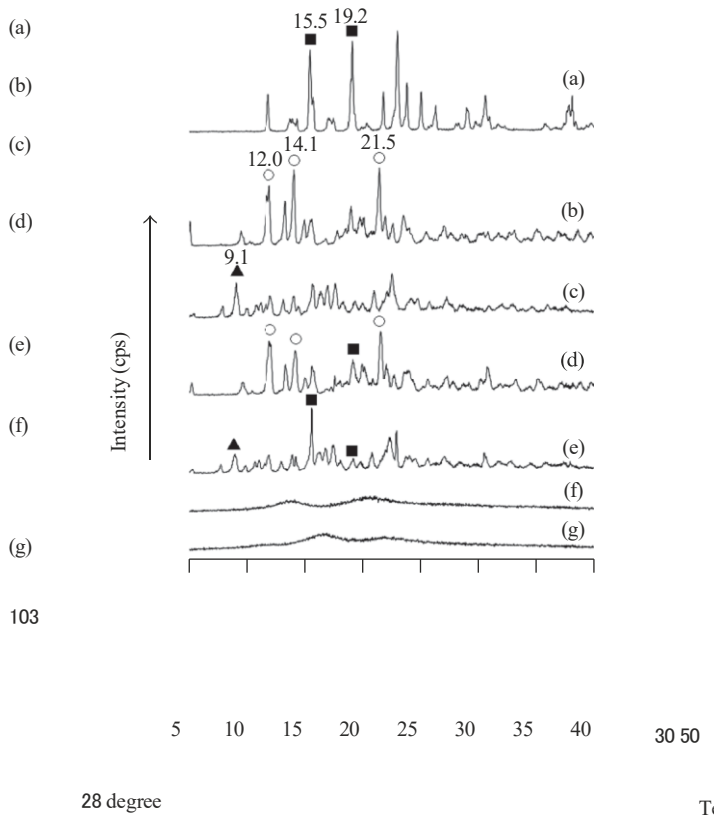


FIGURE 2: PXRD patterns of MT/$\alpha$CD and MT/$\gamma$CD systems. (a) MT intact, (b) $\alpha$CD, (c) $\gamma$CD, (d) PM (MT/$\alpha$CD = 1/1), (e) PM (MT/$\gamma$CD = 1/1), (f) FD (MT/$\alpha$CD = 1/1), (g) FD (MT/$\gamma$ CD = 1/1). ∎: MT original, I: $\alpha$CD original, : $\gamma$ CD original.

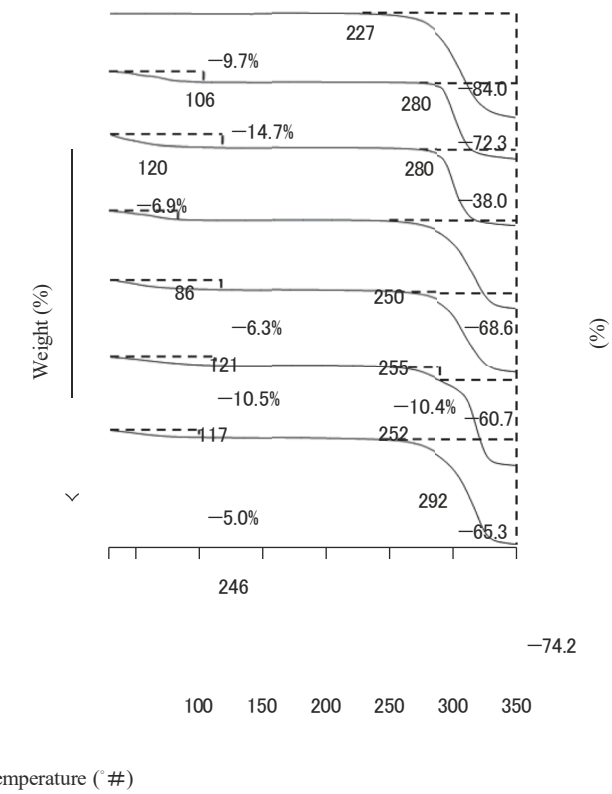


FIGURE 3: TG curves of MT/$\alpha$CD and MT/$\gamma$CD systems. (a) MT, (b) $\alpha$CD, (c) $\gamma$CD, (d) PM (MT/$\alpha$CD = 1/1), (e) PM (MT/$\gamma$CD = 1/1), (f) FD (MT/$\alpha$CD = 1/1), (g) FD (MT/$\gamma$CD = 1/1).

$\alpha$CD exhibited characteristic diffraction peaks at $2\theta$ = 12.0°, 14.1°, 21.52°. The PM (MT/$\alpha$CD) exhibited diffraction peaks derived from $\alpha$CD at $2\theta$ = 12.0°, 14.1°, 21.5° and MT at $2\theta$ = 19.2°. However, FD (MT/$\alpha$CD) exhibited a halo pattern.

$\gamma$CD exhibited a characteristic diffraction peak at $2\theta$ = 9.1°. The PM (MT/$\gamma$CD) exhibited diffraction peaks derived from $\gamma$CD at $2\theta$ = 9.10° and MT at $2\theta$ = 15.5° and 19.16°. However, FD (MT/$\gamma$CD) exhibited a halo pattern similar to that of FD (MT/$\alpha$CD) and an amorphous state was observed. An amorphous state observed during the PXRD measurement of a solid dispersion of CD and a guest molecule suggests that there is a possibility that CD and the guest molecule formed an inclusion complex [9, 10]. From this fact, we presumed that some interaction occurred in the crystalline state during the freeze-drying preparation of FD (MT/$\alpha$CD) and FD (MT/$\gamma$CD).

4.2. *TG-DTA*. An amorphous state was observed in FD

(MT/$\alpha$CD) and FD (MT/$\gamma$CD) during the PXRD measure- ment. Therefore, a TG-DTA measurement was performed to confirm the thermal behavior (Figures 3 and 4). For the intact MT, thermal weight reduction was observed around 227°C. Conversely, a thermal weight decrease was observed at 252°C and 246°C for FD (MT/$\alpha$CD) and FD (MT/$\gamma$CD). In addition, in the intact MT, an endothermic peak owing to the melting point of MT was confirmed around 142°C. Even in the PM (MT/$\alpha$CD) and PM (MT/$\gamma$CD), an endothermic peak owing to the melting point of MT was observed around 141°C. However, an endothermic peak owing to the melting point of MT was not observed in FD (MT/$\alpha$CD) and FD (MT/$\gamma$CD). The increase in the thermal weight reduction temperature

Temperature ( #)

FIGURE 4: DTA curves of MT/$\alpha$CD and MT/$\gamma$CD systems. (a) MT, (b) $\alpha$CD, (c) $\gamma$CD, (d) PM (MT/$\alpha$CD = 1/1), (e) PM (MT/$\gamma$CD = 1/1), (f) FD (MT/$\alpha$CD = 1/1), (g) FD (MT/$\gamma$CD = 1/1).

and the disappearance of the endothermic peak of the guest molecule indicated that an inclusion complex made of CD and the guest molecule was formed [11, 12]. These changes in thermal behavior suggested intermolecular interactions in MT/$\alpha$CD and MT/$\gamma$CD lyophilizates. Incidentally, there was no change in the results of PXRD and TG-DTA measurement after a month of preparation of FD (MT/$\alpha$CD) and FD

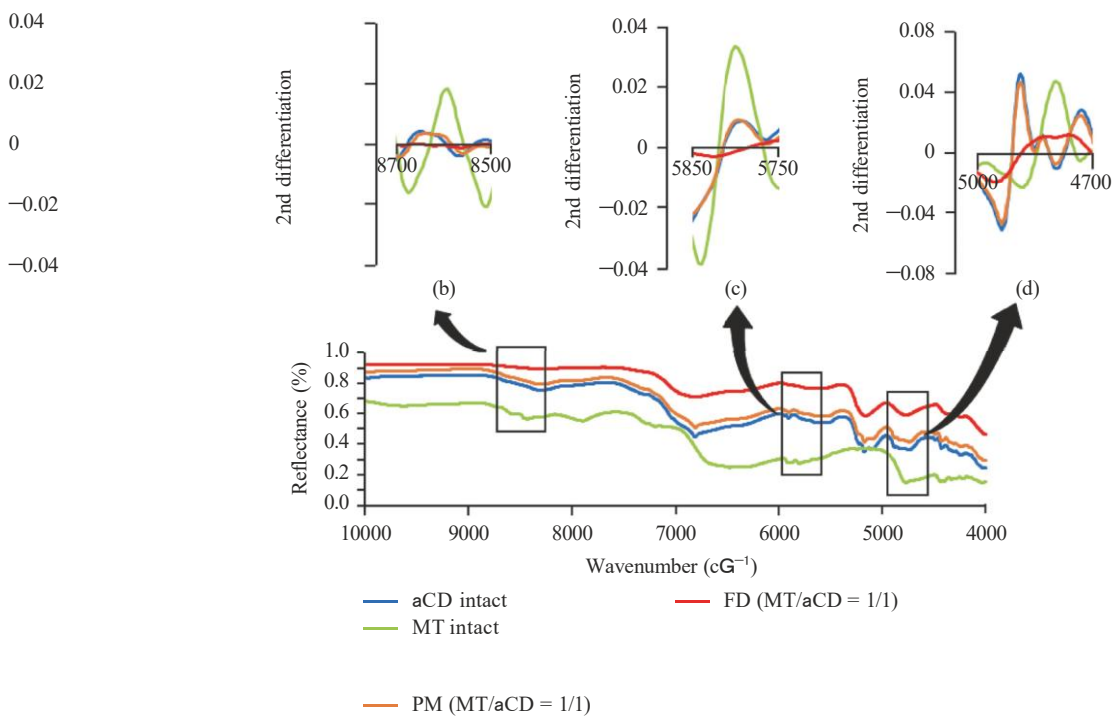


(a)

FIGURE 5: NIR absorption spectra of MT/$\alpha$CD systems and second-differentiation NIR absorption spectra of MT/$\alpha$CD systems ((b) alkyl group, (c) alkyl group, and (d) hydroxy group).

(MT/$\gamma$CD) (not shown data). Therefore, the freeze-dried product (MT/$\alpha$CD and MT/$\gamma$CD) presume is stable.

*4.3. NIR.* PXRD measurement and TG-DTA measurement suggested inclusion complex formation in FD (MT/$\alpha$CD) and FD (MT/$\gamma$CD). Therefore, to verify the detailed intermolec- ular interaction, the NIR absorption spectrum was measured (Figures 5 and 6).

The results of the NIR measurement indicated that the -OH group was observed around 4800 $cm^{-1}$ [13] and 6660 $cm^{-1}$–7140 $cm^{-1}$ [14]. In addition, the -$CH_2$ group was observed around 5800 $cm^{-1}$ [15] and 8145 $cm^{-1}$–9153 $cm^{-1}$ [16]. From the results of the NIR measurement, a peak derived from an -OH group appeared around 4800 $cm^{-1}$ and that from a -$CH_2$ group appeared around 5800 $cm^{-1}$ and 8600 $cm^{-1}$ for MT. In $\alpha$CD alone, a peak derived from an - OH group appeared around 4900 $cm^{-1}$ (Figure 5(a)). In the second derivative spectrum, the peak of the -$CH_2$ group around 8600 $cm^{-1}$ (Figure 5(b)) and 5800 $cm^{-1}$ (Figure 5(c)) of MT was broadened in FD (MT/$\alpha$CD). In addition, the peak derived from the -OH group around 4800 $cm^{-1}$ of MT and the -OH group around 4900 $cm^{-1}$ of $\alpha$CD was broadened (Figure 5(d)). A broadened or shifted peak in the NIR measurement indicated that there were intermolecular interactions between the drug and functional group [17]. This suggested that there were intermolecular interactions between the -$CH_2$ group and -OH group of MT and the -OH group of $\alpha$CD in FD (MT/$\alpha$CD).

In addition, in $\gamma$CD alone, a peak derived from the -OH group appeared around 7000 $cm^{-1}$ (Figure 6(a)). In the results of the second derivative spectrum, the peak of the -OH group around 4800 $cm^{-1}$ (Figure 6(e)) and the peak of -$CH_2$ group around 8600 $cm^{-1}$ (Figure 6(b)) and 5800 $cm^{-1}$ (Figure 5(d)) for MT were broadened in FD (MT/$\gamma$CD).

In addition, the peak derived from the -OH group around 7000 $cm^{-1}$ of $\gamma$CD shifted to the higher wave number (Figure 6(c)). This suggested that there were intermolecular interactions between the -$CH_2$ group and the -OH group in MT and the -OH group in $\gamma$CD in FD (MT/$\gamma$CD).

Miglitol has a -$CH_2$ group at the 6th position in its side chain and at a cyclic structure. Therefore, in the NIR measurement, it is impossible to determine whether the -$CH_2$ group is of the cyclic structure or the 6th position in the side chain. Therefore, detailed examination by 2D-NMR measurement is necessary.

*4.4. $^1$H-$^1$H NOESY NMR Spectroscopy.* NIR measurement indicated an intermolecular interaction between the -$CH_2$ and -OH group of MT and the -OH group of $\alpha$CD and between the -$CH_2$ and -OH group of MT and the -OH group of $\gamma$CD. Therefore, the detailed intermolecular interaction was further evaluated. First, $^1$H-NMR measurement of MT alone was conducted to confirm the attributions of MT. The results indicated that the -CH (h) of MT exhibited two peaks at 3.62 ppm ($h_1$) and 3.72 ppm ($h_2$) (Figure 7). Thereafter, $^1$H- $^1$H NOESY NMR spectroscopy measurement was performed (Figures 8 and 9). In FD (MT/$\alpha$CD), cross peaks were observed between the peak for the -CH ($h_2$: 3.72 ppm) in MT and the H-3 (3.76 ppm) protons in $\alpha$CD (Figure 8). In general, it has been reported that by observing H-3, 5, and 6 protons of the CD cavity and protons of the guest molecule using $^1$H-$^1$H-NMR, the structure of the inclusion complex

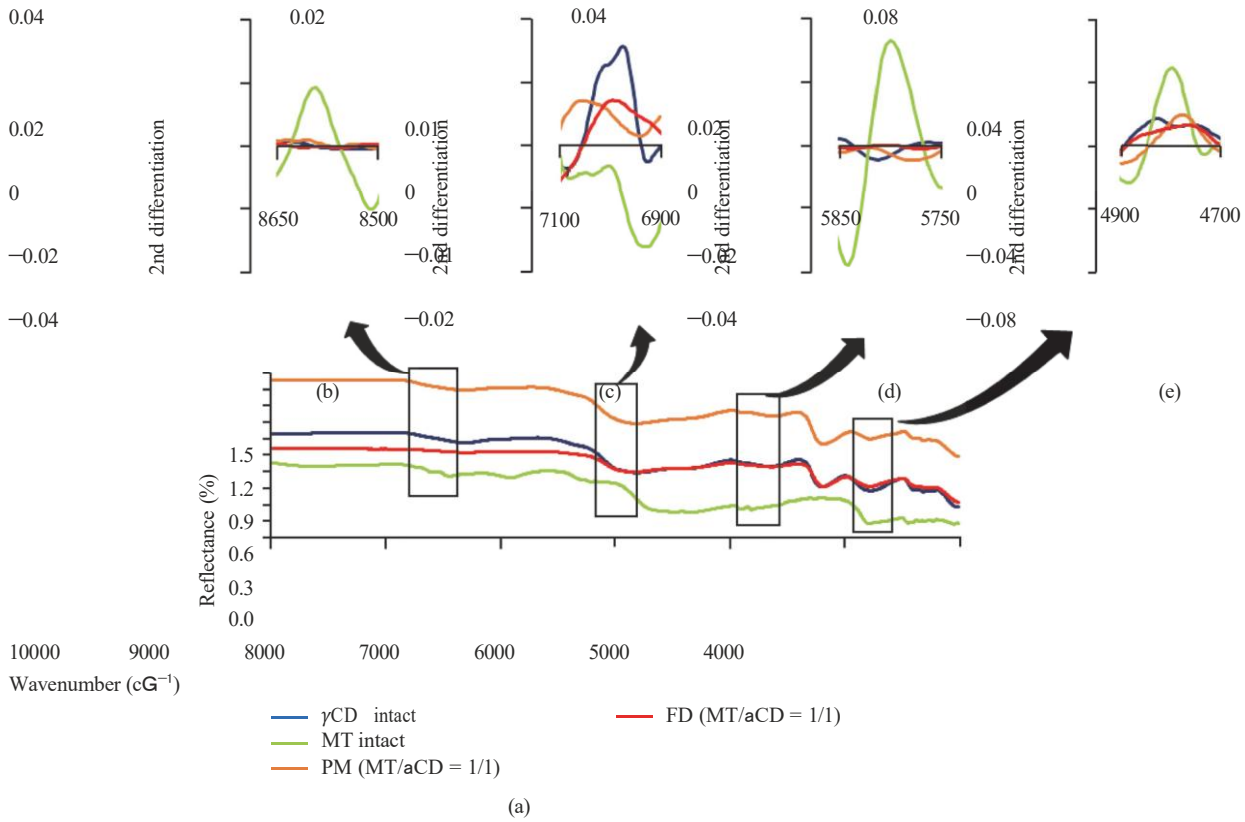


FIGURE 6: NIR absorption spectra of MT/γCD systems and second-differentiation NIR absorption spectra of MT/γCD systems ((b) alkyl group of MT, (c) hydroxy group of γCD, (d) alkyl group of MT, and (e) hydroxy group of MT).

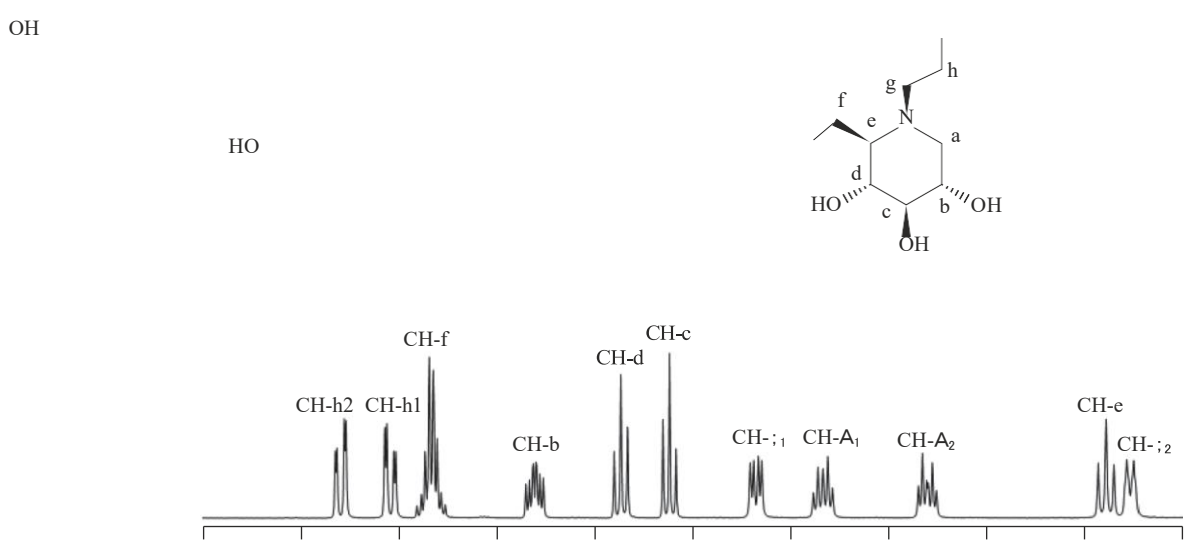

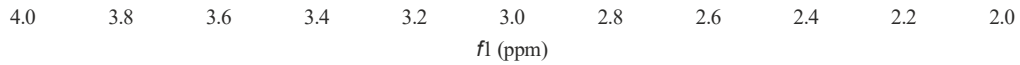


FIGURE 7: Proton-NOESY NMR spectra of MT in $D_2O$.

can be elucidated [18]. In addition, from this result, a cross peak between H-3 showing the wide edge of CD and the -CH ($h_2$: 3.72 ppm) in MT was observed in FD (MT/$\alpha$CD). This suggested that the inclusion complex made of $\alpha$CD and MT was in a form covering the alkyl group of MT from the cavity of a wide edge of CD with respect to the alkyl group of the
-CH (h) of MT.Additionally, in FD (MT/$\gamma$CD), cross peaks were observed between the peak for -CH ($h_1$: 3.62 ppm, $h_2$: 3.72 ppm) of MT and the H-3 (3.72 ppm) and H-6 (3.65 ppm) protons of $\gamma$CD (Figure 9). From this result, a cross peak between H-3 showing the wide edge of CD and -CH ($h_2$: 3.72 ppm) of MT was observed in FD (MT/$\gamma$CD). This suggested that the inclusion complex made of $\gamma$CD and MT

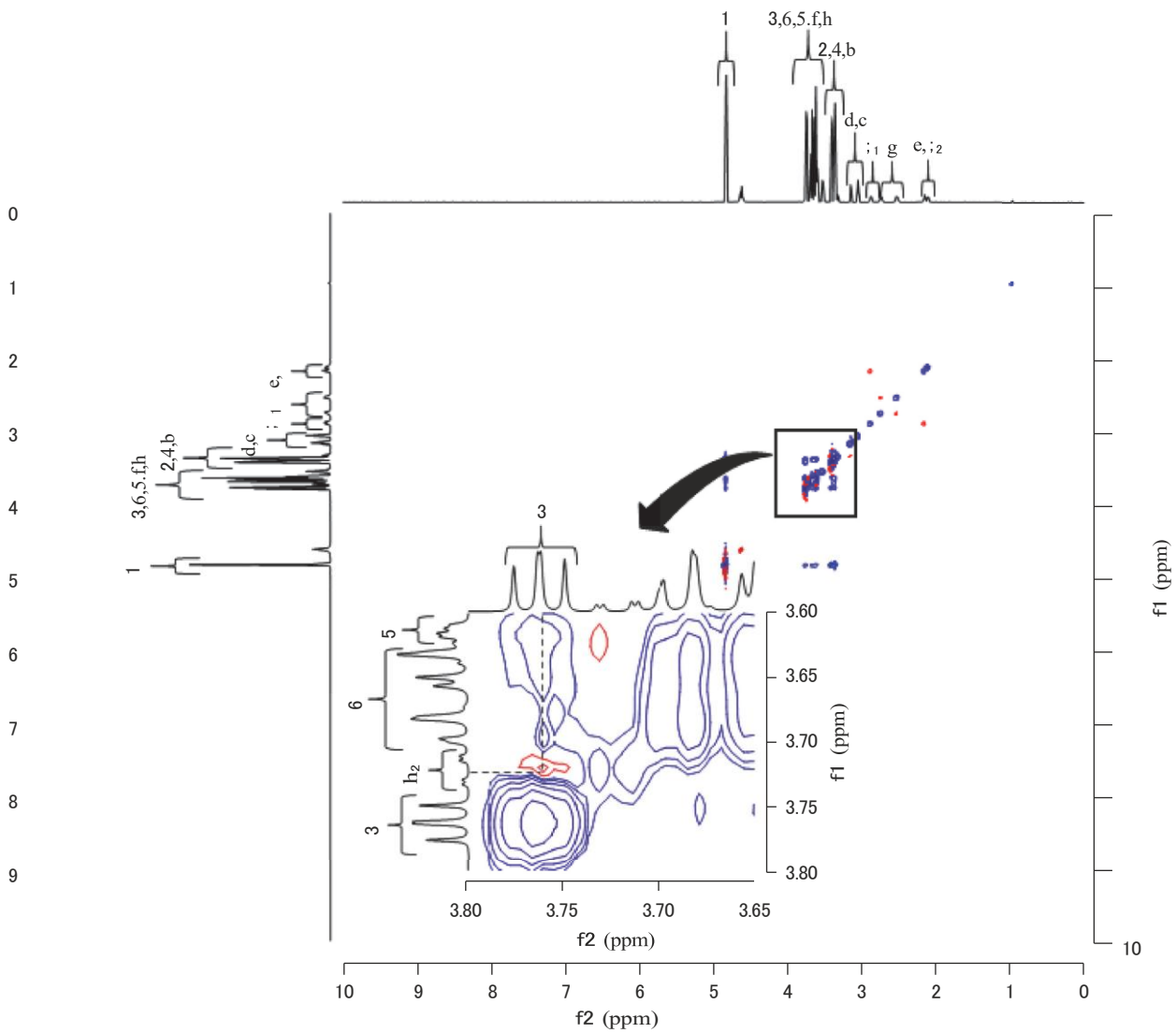


FIGURE 8: $^1$H-$^1$H -NOESY NMR spectra of MT/$\alpha$CD system.

included a form covering the alkyl group of MT from the cavity of a wide edge of CD with respect to the

alkyl group of the -CH (h) in MT. This confirmed that the inclusion complex with MT was similar between that with $\alpha$CD and that with $\gamma$CD with different cavity diameters.

*4.5. $\alpha$-Glucosidase Activity Inhibition Test.* Inclusion com- plex formation was confirmed for FD (MT/$\alpha$CD) and FD (MT/$\gamma$CD). Because deterioration of bioactivity is an area of concern for inclusion preparations, the MT in inclusion complexes was tested for $\alpha$-glucosidase activity (Table 1). For intact MT, a 51.2% inhibition of $\alpha$-glucosidase activity was observed. In addition, FD (MT/$\alpha$CD) and FD (MT/$\gamma$CD) exhibited inhibition rates of 56.2% and 56.6%, respectively, which was similar to the inhibition rates observed with intact MT. Inhibition of $\alpha$-glucosidase activity was not observed in $\alpha$CD or $\gamma$CD. This indicated that the $\alpha$-glucosidase inhibitory activity depended on the concentration of MT and confirmed

TABLE 1: Inhibitory activities $\alpha$-glucosidase and $\alpha$-amylase.

| | Percentage of inhibition | |
|---|---|---|
| | $\alpha$-Glucosidase | $\alpha$-Amylase |
| MT | 51.2 ± 7.3 | — |
| $\alpha$CD | — | 4.4 ± 2.5 |
| $\gamma$CD | — | 3.1 ± 1.1 |
| PM (MT/$\alpha$CD) | 51.5 ± 10.2 | 0.1 ± 0.8 |
| PM (MT/$\gamma$CD) | 56.2 ± 6.8 | 3.2 ± 2.2 |
| FD (MT/$\alpha$CD) | 49.9 ± 7.4 | 2.8 ± 1.1 |
| FD (MT/$\gamma$CD) | 56.6 ± 4.9 | 1.3 ± 2.6 |

Values are expressed as mean ± standard deviation ($n$ = 3). Each data value showed statistically significant difference at $p$ value < 0.05 using Turkey's multiple comparison tests. that the $\alpha$-glucosidase inhibitory activity of MT in the inclusion complex was sufficiently maintained.

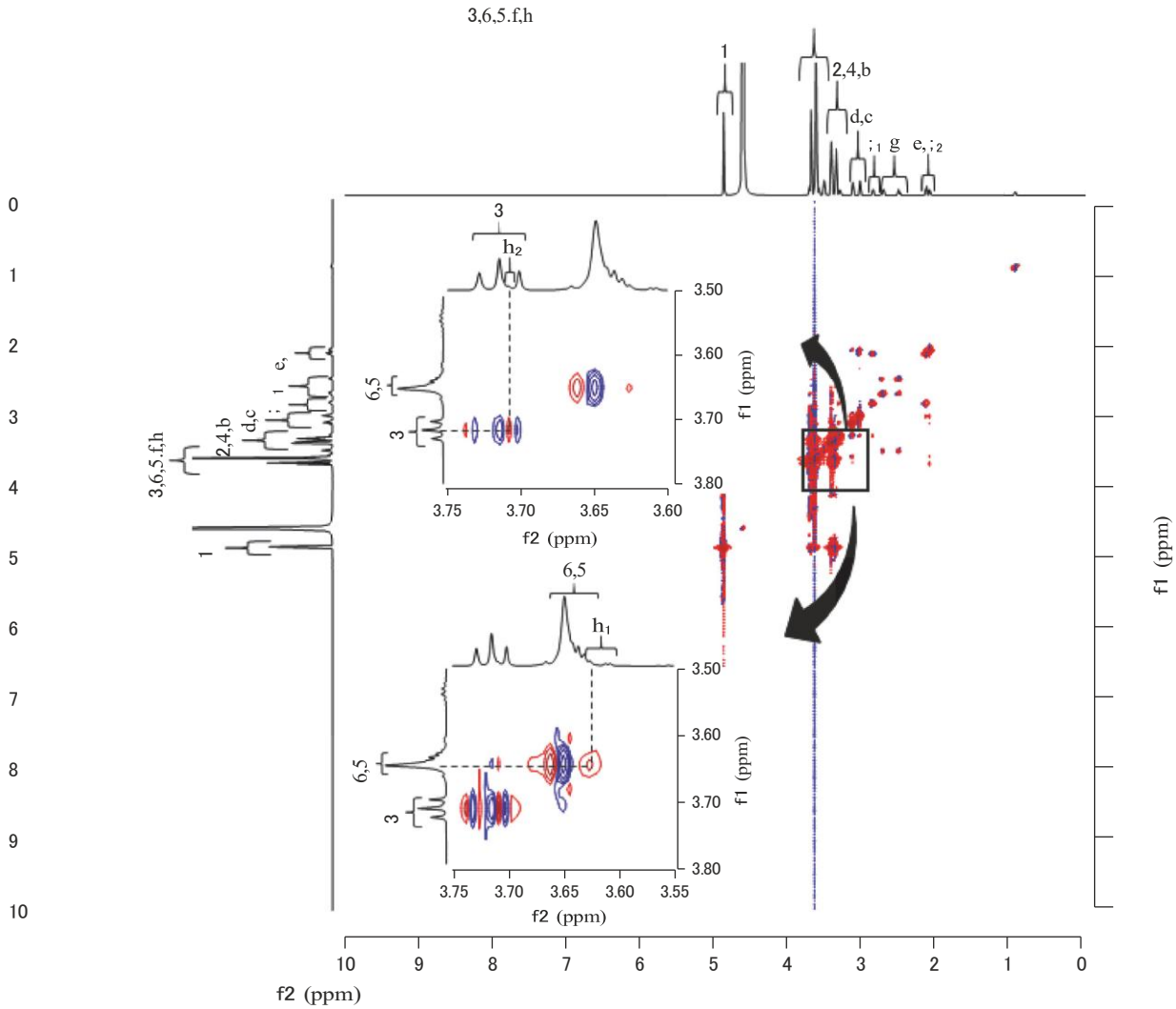


FIGURE 9: $^{1}H$-$^{1}H$ -NOESY NMR spectra of MT/$\gamma$CD system.

4.6. *α-Amylase Activity Inhibition Test.* αCD has been reported to inhibit α-amylase activity. To confirm the influ- ence on the inhibition of α-amylase activity by the formation of these complexes, an α-amylase activity inhibition test was conducted (Table 1). Intact MT did not inhibit α-amylase activity. Conversely, αCD and γCD exhibited inhibition rates of 4.41% and 3.10%. In addition, FD (MT/αCD) and FD (MT/γCD) exhibited inhibition rates of 3.21% and 1.29%, which were almost equal to the inhibition rates observed with
αCD and γCD alone. This was due to inhibition of α-amylase activity by both αCD and γCD and indicated that the α- amylase inhibitory activity of αCD and γCD in the prepared complex was sufficiently maintained. The dose of CD used to prepare the FD was very small compared with the dose reported to affect the inhibition of α-amylase activity [19]. Therefore, the α-amylase activity rate was very low. In the future, it will be necessary to confirm these results under different conditions. Further investigation should evaluate the effects on blood sugar in animal studies using these preparations.n this study, MT/αCD and MT/γCD were evaluated, but a preparation containing MT/βCD should also be evaluated. However, MT/βCD is not as easily prepared by freeze-drying as MT/αCD and MT/γCD. The cavity of βCD is hydrophobic compared to αCD and γCD. On the other hand, MT of a drug used as a guest molecule in this study is a water- soluble drug. Therefore, MT/βCD inclusion complex might not be confirmed. In the future, we plan to develop a better preparation method.

## 5. Conclusion

In this study, we prepared MT/αCD complex and MT/γCD complex using a freeze-drying method. In addition, it was confirmed that the structure of the inclusion complex differed depending on the size of the CD ring. Furthermore, we found that there was no influence on the inhibition of α-glucosidase or α-amylase activity depending on the preparation process used for the FD.

## References

[1] "Healthy lifestyle behaviors and all-cause mortality among adults in the United States," by E. S. Ford, M. M. Bergmann, H. Boeing, C. Li, and S. Capewell, Preventive Medicine, vol. 55, no. 1, pp. 23–27, 2012.
[2] R. Koukiekolo, V. Desseaux, Y. Moreau, G. Marchis-Mouren, and M. Santimone, "Pig pancreatic amylase mechanism: suppression of amylose and maltopentaose hydrolysis by "Cyclodextrins of the α, β, and γ types," European Journal of Biochemistry, vol. 268, no. 3, pp. 841–848, 2001.
[3] "Effect of cyclodextrin on postprandial blood glucose and triglycerides," International Journal Pharmacy, vol. 6, no. 3, pp. 13–19, 2016, M. Sugahara, Y. Inoue, I. Murata et al.
[4] A. H. Alomrani, G. A. Shazly, A. A. A. F. Amara, and M. M. Badran, "Itraconazole-hydroxypropyl-β-cyclodextrin loaded deformable liposomes: in vitro skin penetration studies and antifungal efficacy using Candida albicans as model," Colloids and Surfaces B: Biointerfaces, vol. 121, pp. 74–81, 2014. Chemical & Pharmaceutical Bulletin, vol. 62, no. 8, pp. 786–792, 2014; Y. Inoue, N. Sekiya, K. Katayama, et al., "Stabilizing effect of β-cyclodextrin on Limaprost, a PGE1 derivative, in Limaprost alfadex tablets (Opalmon®) in highly humid conditions."
[6] J. Szejtli and L. Szente, "Using cyclodextrins to eliminate an unpleasant, bitter taste from medications and foods," European Journal of Pharmaceutics and Biopharmaceutics, vol. 61, no. 3, pp. 115–125, 2005.
[7] J.-Y. Yang, J.-H. Park, N. Chung, and H.-S. Lee, "Osmanthus fragrans constituents and structural analogues against advanced glycation end products, α-amylase, α-glucosidase, and oxidative stress," Scientific Reports, vol. 7, Article ID 45746, 2017.

[8] "In-vitro alpha amylase inhibitory activity of the leaf extracts of adenanthera pavonina," BMC Complementary and Alternative Medicine, vol. 16, no. 1, Article ID 466, 2016, M. N. Wickramaratne, J. C. Punchihewa, and D. B. M. Wickramaratne.
[9] "Characterization of an inclusion complex of cholesterol and hydroxypropyl-$\beta$-cyclodextrin," European Journal of Pharmaceutics and Biopharmaceutics, vol. 46, no. 3, pp. 355–360, 1998, R. O. Williams III, V. Mahaguna, and M. Sriwongjanya.
[10] "Analysis of freeze-dried quercetin-cyclodextrin binary systems by DSC, FT-IR, X-ray" by T. Pralhad and K. Rajendrakumardiffraction and SEM analysis," *Journal of Pharmaceutical and Biomedical Analysis*, vol. 34, no. 2, pp. 333–339, 2004.

[1] L. P. Fernandes, Z. É hen, T. F. Moura, C. Nova´k, and J. Sztatisz, "Characterization of Lippia sidoides oil extract-b-cyclodextrin complexes using combined thermoanalytical techniques," *Jour- nal of Thermal Analysis and Calorimetry*, vol. 78, no. 2, pp. 557– 573, 2004.

[2] P. Guo, Y. Su, Q. Cheng, Q. Pan, and H. Li, "Crystal struc- ture determination of the $\beta$-cyclodextrin-p-aminobenzoic acid inclusion complex from powder X-ray diffraction data," *Carbo- hydrate Research*, vol. 346, no. 7, pp. 986–990, 2011.

[3] R. G. Dambergs, A. Kambouris, L. Francis, and M. Gishen, "Rapid analysis of methanol in grape-derived distillation prod- ucts using near-infrared transmission spectroscopy," *Journal of Agricultural and Food Chemistry*, vol. 50, no. 11, pp. 3079–3084, 2002.

[4] T. A. Lestander, M. Rudolfsson, L. Pommer, and A. Nordin, "NIR provides excellent predictions of properties of biocoal from torrefaction and pyrolysis of biomass," *Green Chemistry*, vol. 16, no. 12, pp. 4906–4913, 2014.

[5] A. D. Zotte, P. Berzaghi, L.-M. Jansson, and I. Andrighetto, "The use of near-infrared reflectance spectroscopy (NIRS) in the prediction of chemical composition of freeze-dried egg yolk and discrimination between different n − 3 PUFA feeding sources," *Animal Feed Science and Technology*, vol. 128, no. 1-2, pp. 108– 121, 2006.

[6] V. Gaydou, J. Kister, and N. Dupuy, "Evaluation of multi- block NIR/MIR PLS predictive models to detect adulteration of diesel/biodiesel blends by vegetal oil," *Chemometrics and Intelligent Laboratory Systems*, vol. 106, no. 2, pp. 190–197, 2011.

[7] S. Duri and C. D. Tran, "Supramolecular composite materials from cellulose, chitosan, and cyclodextrin: facile preparation and their selective inclusion complex formation with endocrine disruptors," *Langmuir*, vol. 29, no. 16, pp. 5037–5049, 2013.

[8] A. Lis-Cieplak, J. Sitkowski, and W. Kolodziejski, "Comparative proton nuclear magnetic resonance studies of amantadine complexes formed in aqueous solutions with three major cyclodextrins," *Journal of Pharmaceutical Sciences*, vol. 103, no. 1, pp. 274–282, 2014.

[9] N. Oudjeriouat, Y. Moreau, M. Santimone, B. Svensson, G. Marchis-Mouren, and V. Desseaux, "On the mechanism of
$\alpha$-amylase. Acarbose and cyclodextrin inhibition of barley amylase isozymes," *European Journal of Biochemistry*, vol. 270, no. 19, pp. 3871–3879, 2003.